Review of the IDEA Drift Chambers

Riccardo Farinelli

Co-Liaison from gaseous detector community to the ECFA WG3

Outline

- IDEA drift chamber design and requirements
- Mechanics, electronics and aging
- Simulation
- Cluster counting
- Performance evaluation
- Machine background

Bibliography

https://agenda.infn.it/event/28874/contributions/169552/attachments/94486/129350/20220708_idea_gaudio.pdf
The IDEA detector concept for FCC-ee and CepC - G. Gaudio - Jul 2022

https://indico.slac.stanford.edu/event/7467/contributions/5947/attachments/2818/7991/IDEA_Full%20simulation%20in%20Key4hep_Armin%20Ilg.pdf
Full simulation of the IDEA detector at FCC-ee using the Key4hep framework - A. Ilg - May 2023

https://arxiv.org/pdf/2107.04509.pdf
Exploring requirements and detector solutions for FCC-ee - P. Azzi - Jul 2021

https://indico.cern.ch/event/1307378/contributions/5720993/attachments/2789172/4864168/240129_Annecy_Phys_Week__MDI_Mboscolo.pdf
PROGRESS AND PROSPECTS ON THE MDI STUDY - M. Boscolo - Jan 2024

https://indico.cern.ch/event/1307378/contributions/5720994/attachments/2789155/4863577/Annecy2024-PhysPerformance.pdf
Detector Requirements and case studies - P. Azzi - Jan 2024

https://indico.cern.ch/event/1307378/contributions/5723982/attachments/2790243/4866662/2024-01-30_PID_FCC-Physics-WS.pdf
PID performances and the Bs→DsK analysis with the IDEA detector - A. Coccaro - Jan 2024

https://indico.cern.ch/event/1307378/contributions/5727842/attachments/2789988/4865303/primavera_FCCFranceworkshop_Jan2024v1.pdf
Progress and Developments on the IDEA Drift Chamber - M. Primavera - Jan 2024

https://iopscience.iop.org/article/10.1088/1748-0221/11/07/P07011/pdf
Single-hit resolution measurement with MEG II drift chamber prototypes - A. Baldini - Jul 2016

https://agenda.infn.it/event/28874/contributions/169548/attachments/94400/129169/Walaa%20IDEA%20DCH.pdf
The Tracking performance for the IDEA drift chamber - W. Elmetenawee - Jul 2022

https://agenda.infn.it/event/28874/contributions/169554/attachments/94326/129042/cc_ichep_cuna.pdf
Particle identification with the cluster counting technique in the IDEA drift chamber - F. Cuna - Jul 2020

Bibliography

https://arxiv.org/pdf/1801.04688.pdf
The design of the MEG II experiment - MEG II - Jan 2018

https://indico.cern.ch/event/1237829/contributions/5609619/attachments/2747195/4780632/Aging%20phenomenon%20in%20BESIII%20drift%20chamber.pdf
Aging phenomenon in BESIII drift chamber - M. Dong - Nov 2023

https://agenda.infn.it/event/28874/contributions/169554/attachments/94326/129042/cc_ichep_cuna.pdf
Particle identification with the cluster counting technique in the IDEA drift chamber - F. Cuna - July 2022

https://arxiv.org/pdf/2105.07064.pdf
Simulation of particle identification with the cluster counting technique - F. Cuna - May 2021

https://indico.cern.ch/event/1307378/contributions/5721002/attachments/2790318/4865947/20240129_fullSim_reco_BrieucFrancois_Annecy_FCC_workshop_v2.pdf
FCC Full Sim and Reco Status and Needs - B. Francois - Jan 2024

https://doi.org/10.1016/j.nima.2022.167734
Implementation of the Cluster Counting and Timing technique on FPGA for the reduction of transferred data and stored information - G. Chiarello - Nov 2022

https://arxiv.org/pdf/2211.12568.pdf
The Tracking performance for the IDEA drift chamber - W. Elmetenawee - Nov 2022

https://arxiv.org/pdf/2006.02378.pdf
The Drift Chamber of the MEG II experiment - G. Tassielli - Jun 2020

https://arxiv.org/pdf/2005.02242.pdf
Commissioning of the MEG II tracker system - M. Chiappini - May 2020

https://meg.web.psi.ch/docs/theses/chiappini_phd.pdf
The construction and commissioning of the ultra low mass MEG II drift chamber for the search of the $\mu^+ \rightarrow e^+\gamma$ decay at branching ratios below 10^{-13} - M. Chiappini - Dec 2019

https://pos.sissa.it/390/877/pdf
A proposal of a drift chamber for the IDEA detector concept for a future e^+e^- collider - G. Tassielli - Aug 2020

IDEA detector

Parameters	
vertex technology	silicon
vertex inner/outer radius (cm)	1.7/34
tracker technology	drift chamber and silicon wrapper
tracker half length (m)	2.0
tracker outer radius (m)	2.0
solenoid field (T)	2.0
solenoid bore radius/half length (m)	2.1/3.0
preshower absorber	lead
preshower R_{min}/R_{max} (m)	2.4/2.5
DR calorimeter absorber	copper
DR calorimeter R_{min}/R_{max} (m)	2.5/4.5
overall height/length (m)	11/13

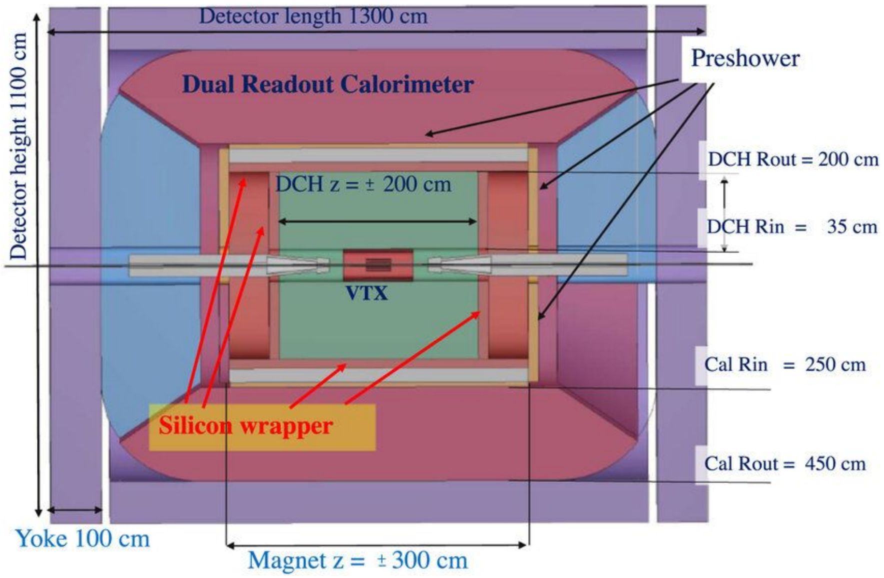

Drift chamber design

Large volume: Radius 0.35-2 m
Length 4m

Coverage: Full stereo **112** co-axial **layers**
Solid angle 97%

Material budget: Barrel 1.6% X_0
Endcap 5.0% X_0
Inner and outer walls of carbon fiber (2x100μm) and foam sandwich

Wires: Sense 20 μm diameter W(Au)
Field 40-50 μm diameter Al(Ag)
Ratio 5:1
Stereo angle 50-250 mrad

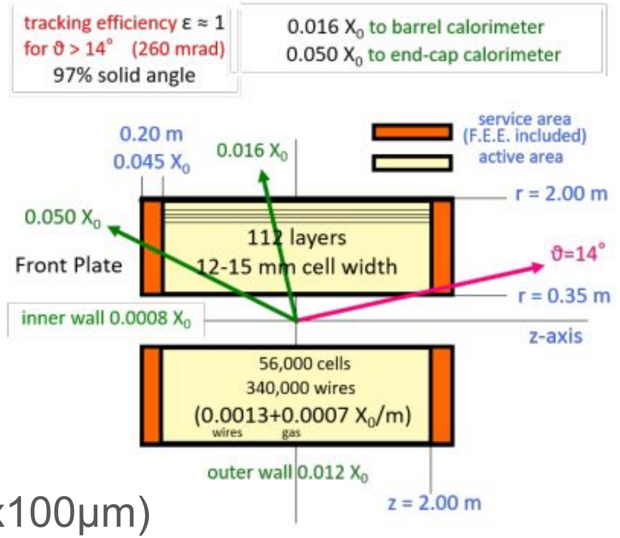

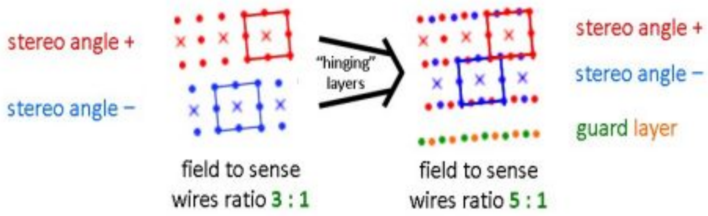

Drift chamber design

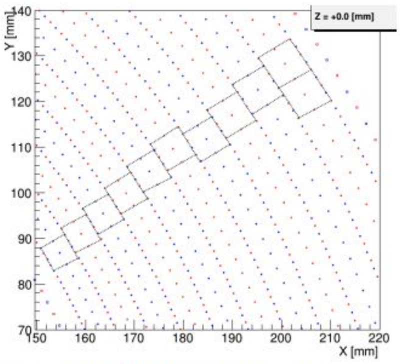

Gas mixture: 90% He – 10% iC_4H_{10}

Granularity: Squared cell dimension 12-14.5 mm
Drift time 350-400 ns

Spatial resolution: $\sigma_{xy} \sim 100\ \mu m$
$\sigma_z \sim 1\ mm$

Momentum resolution: $\sigma(1/pT) \sim 3 \times 10^{-5}\ GeV^{-1} + 0.6 \times 10^{-3}\ /p_T$

Cluster counting: $(\sigma(dNcl/dx)/(dNcl/dx) \approx 2\%$
MIP ionization 12 cm^{-1}

Tungsten in the sense wires is the larger contribution to the material budget.

Drift Chamber pillars

Transparency (1.6% X_0)

High granularity (112 layers)

PID improved (cluster counting)

$$\frac{\Delta p_T}{p_T}|_{res.} \approx \frac{12\,\sigma_{r\phi}\,p_T}{0.3\,B_0 L_0^2}\sqrt{\frac{5}{N+5}}$$

$$\frac{\Delta p_T}{p_T}|_{m.s.} \approx \frac{0.0136\,\mathrm{GeV/c}}{0.3\beta\,B_0 L_0}\sqrt{\frac{d_{tot}}{X_0\,\sin\theta}}$$

Precise tracking achieved together with the vertex detector and the silicon wrapper

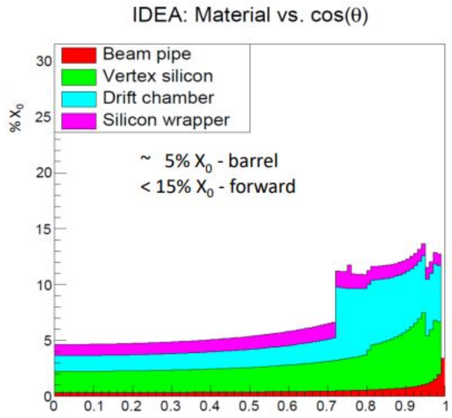

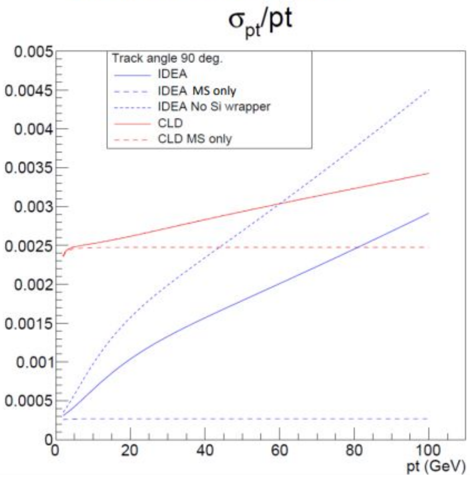

IDEA requirement and benchmark examples: tracking

The following physics processes are used to evaluate the impact of the tracking performance:

ZH, $Z \rightarrow e^+e^-$, $\mu^+\mu^-$ $H \rightarrow \mu^+\mu^-$

measuring mH, $\boldsymbol{\sigma}$(ZH), BR($H \rightarrow \mu^+\mu^-$)

$Z \rightarrow \boldsymbol{\tau}\mu$ for LFV

background $Z \rightarrow \boldsymbol{\tau\tau}$ and sensitivity improves linearly with momentum resolution on the muon

IDEA requirement and benchmark example: PID

PID studies for K/π separation

$B_s \to D_s K$ with $D_s \to \phi\pi$ and $\phi \to KK$

Here the mass spectrum w/o and w/ PID

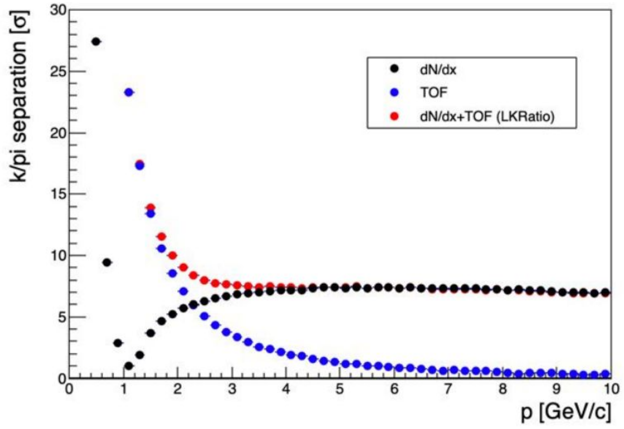

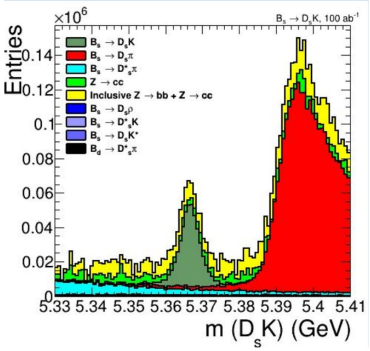

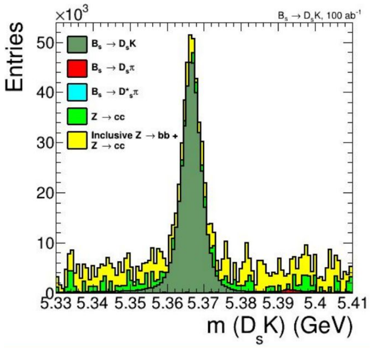

IDEA DCH mechanics

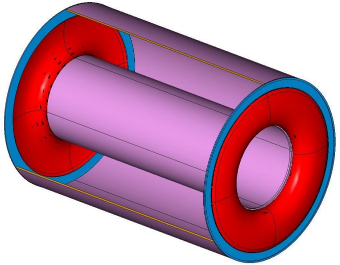

Separated endplates for **mechanics** and **gas sealing**

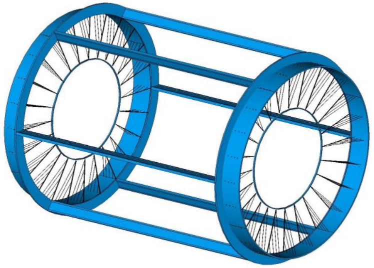

Wiring technique close to MEG-II drift chamber (**feed-through-less**)

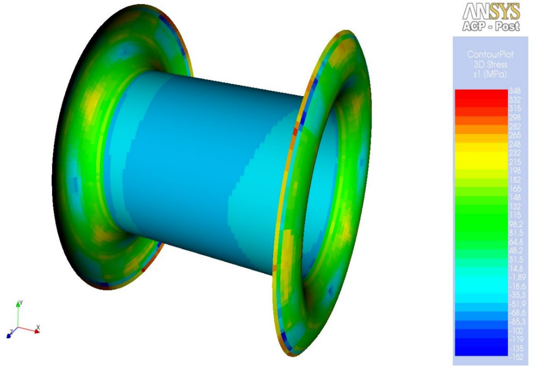

Finite element analysis for the **wire tension recovery scheme**.

IDEA DCH mechanics

Construction a full-size **prototype** (4m long) **is planned** to test different **wire** choices (diameter, material) and the relative **electrostatic stability** and to validate the proposed **tension** recovery **scheme** of the endplates.

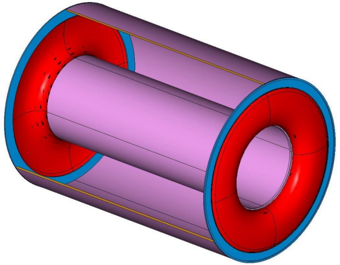

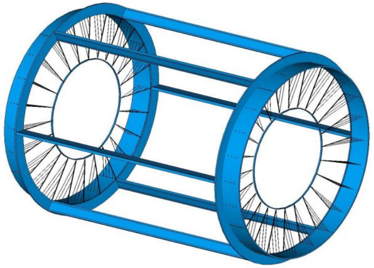

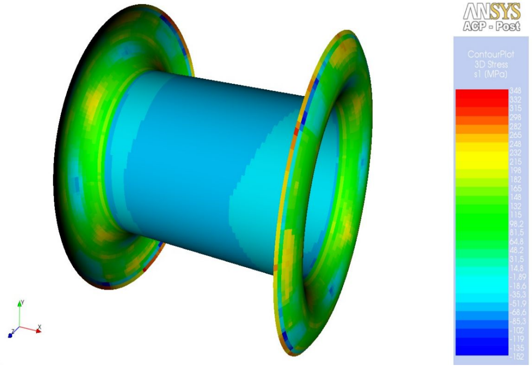

MEG-II DCH mechanics

Feed-through-less technique to reduce the cell dimension

Automatic wiring robot to guarantee the wire positioning and stretching on the PCB

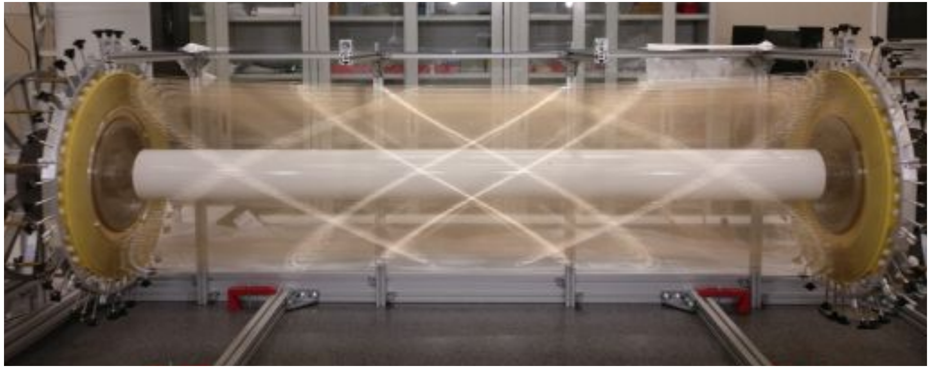

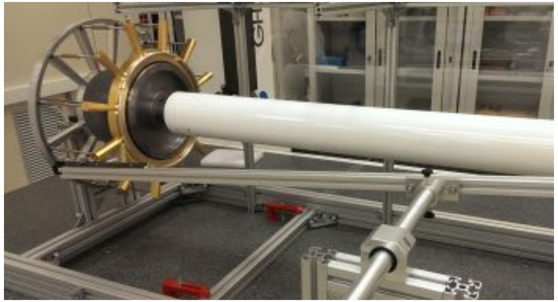

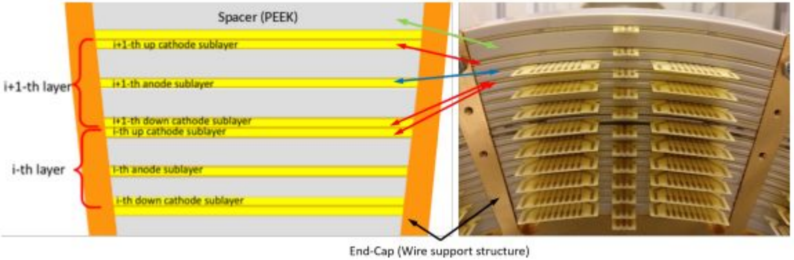

IDEA DCH readout

Cluster counting technique impose severe requirements on the readout.

The arrival times of each individual ionization electrons is measured by the **electronics placed on both sides** of the endcaps.

Readout on both wire ends with a total **drift time of 400ns** and a **digitization** at 14 bits and **2GS/s**.

Online algorithm on FPGA identifies the single ionization peak in the signal needed by the cluster counting to reduce the throughput from 1 Tb/s to 60 Gb/s (R&D ongoing)

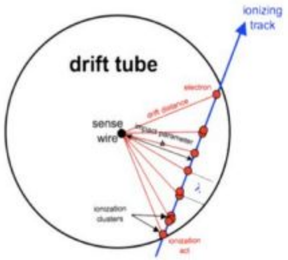

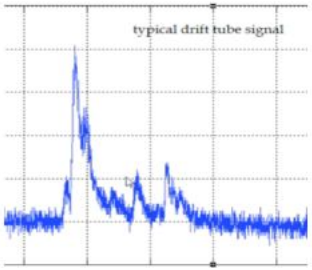

Drift chamber aging

Deposits on the anodes cause a **gain loss** due to the increase in effective diameter of the sense wires.

MEG-II and **BESIII** drift chambers are reported.

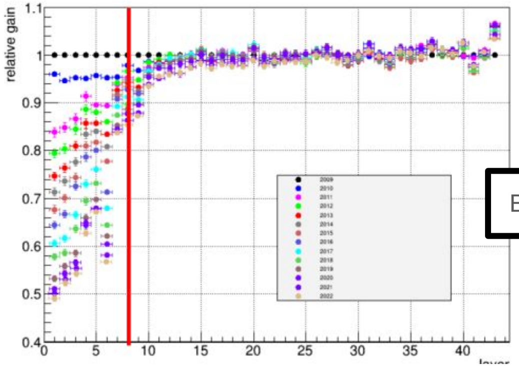

BESIII

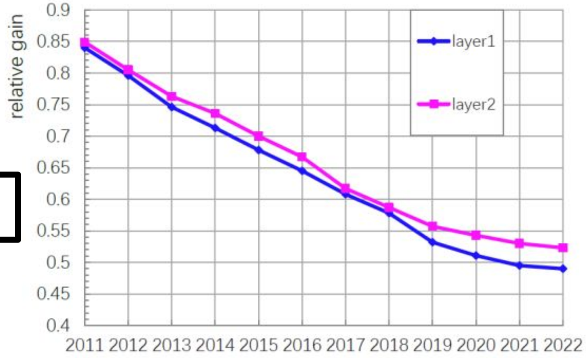

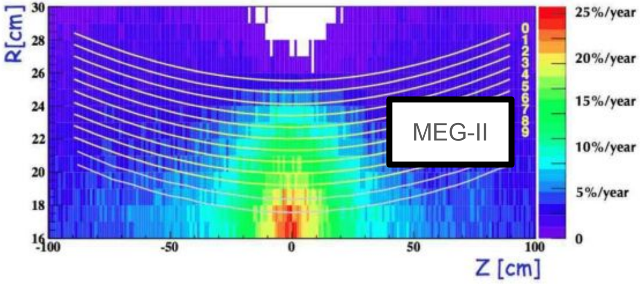

Figure 38 Gain drop in one year of DAQ time.

Aging: MEG-II example

Wire breaking problems arose during MEG-II drift chamber assembly.

Problem was investigated: chemical and mechanical analysis showed that the origin is the chemical corrosion of Al core in presence of **water condensation**.

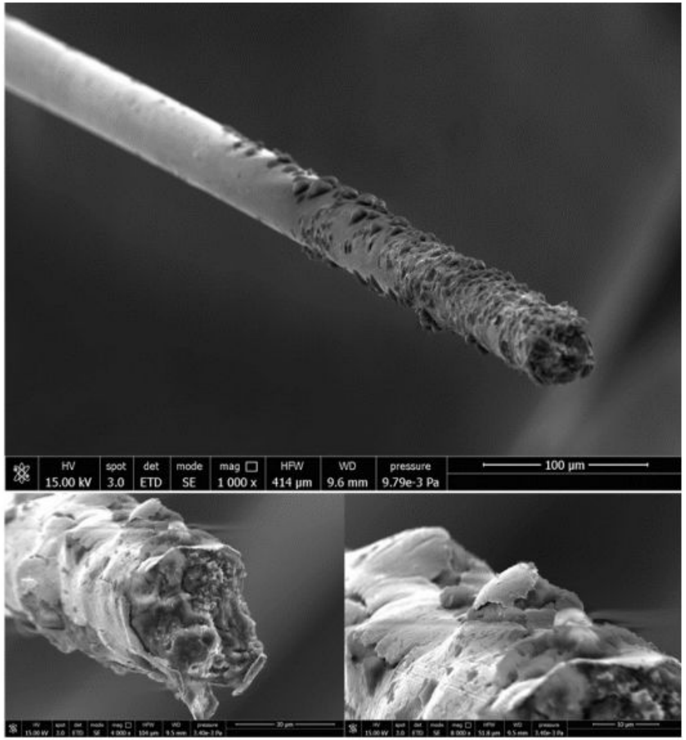

Figure 5.8: SEM images of 2 breaking points.

IDEA DCH simulation

Geant4 and Garfield++ simulations first, then **DD4HEP** implementation are used to evaluate the performance of the DCH

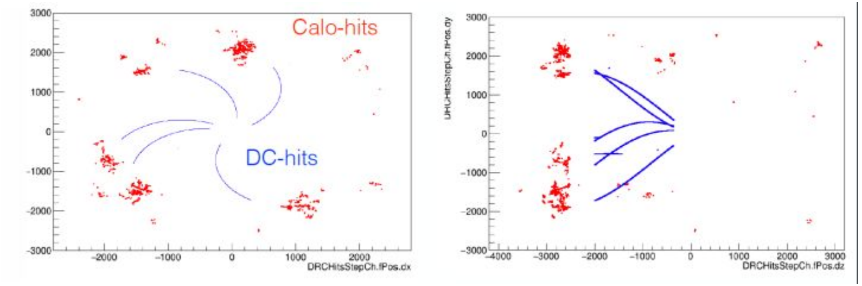

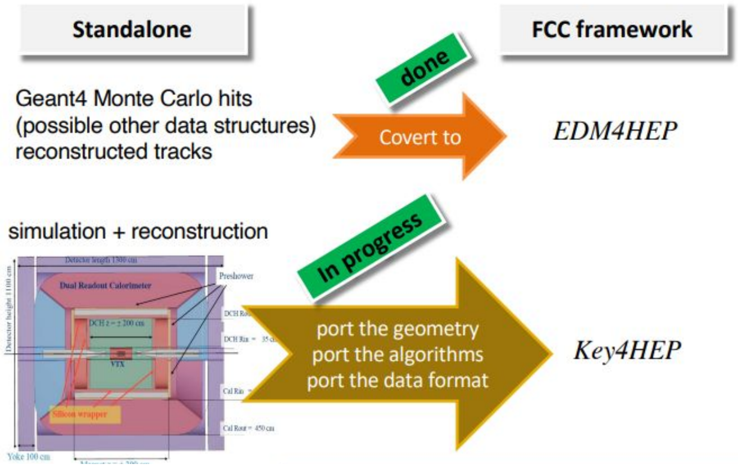

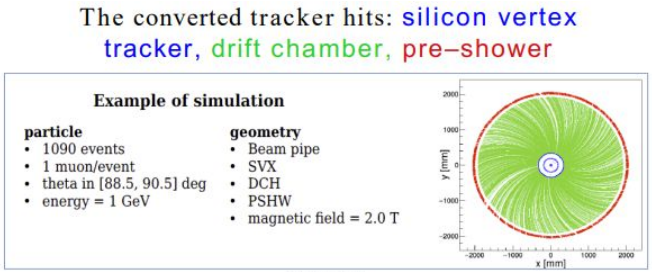

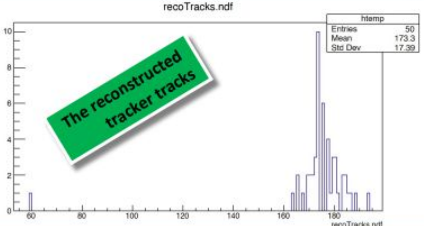

IDEA DCH testbeam

Need to **demonstrate** the ability to **count clusters**: at a fixed **βγ** (e.g. muons at a fixed momentum) count the clusters by doubling and tripling the track length and changing the track angle.

Establish the **limiting parameters** for an efficient cluster counting:
- cluster density (by changing the **gas mixture**)
- space charge (by changing **gas gain**, sense **wire** diameter, track angle)
- gas gain saturation

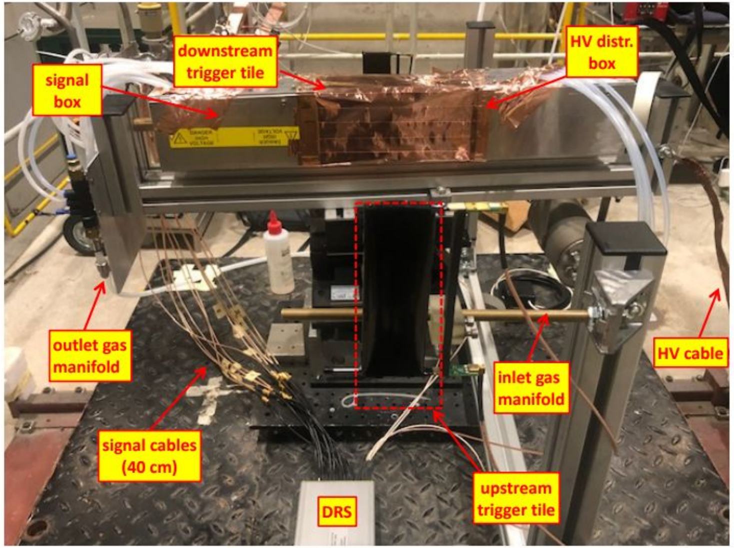

Event display

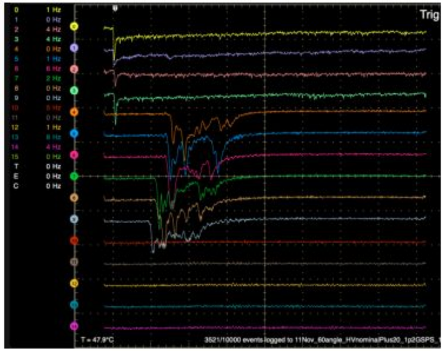

The experimental setup at CERN H8 beam November 2021

Drift tubes pack

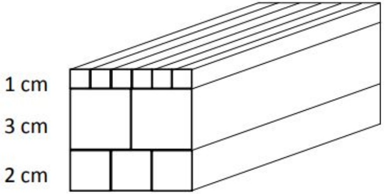

Cluster counting

Counting dNcl/dx (# of ionization acts per unit length) make possible to identify particles (P.Id.) with a better resolution than dE/dx

dE/dx: requires high stability on HV and gas parameters and electronics calibration with truncated mean cut (70-80%) reduces the amount of information.
For n = 112 and a 2m track at 1 atm → σ ≈ 4.3%

CC: Requires fast electronics and sophisticated counting algorithms. It is less dependent on gain stability issues
For δcl = 12./cm for He/iC4H10=90/10 and a 2m track → σ ≈ 2.0%

$$\frac{\sigma_{dE/dx}}{(dE/dx)} = 0.41 \cdot N^{-0.43} \cdot \left(L_{track}[m] \cdot P[atm]\right)^{-0.32}$$

Empirical parametrization

P. Reak and A.H. Walenta, IEEE Trans. Nucl. Sci. NS-27 (1980) 54

$$\frac{\sigma_{dN_{cl}/dx}}{(dN_{cl}/dx)} = \left(\delta_{cl} \cdot L_{track}\right)^{-1/2} = N_{cl}^{-1/2}$$

Poisson

Cluster counting in simulation

Analytical calculations predict excellent K/p separation over the full range of momenta except 0.85<p<1.05 GeV

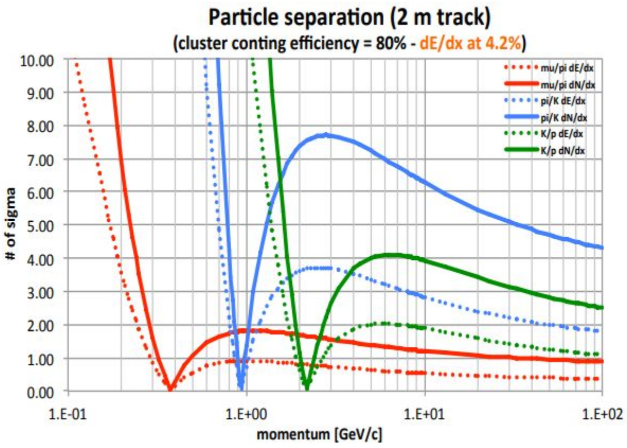

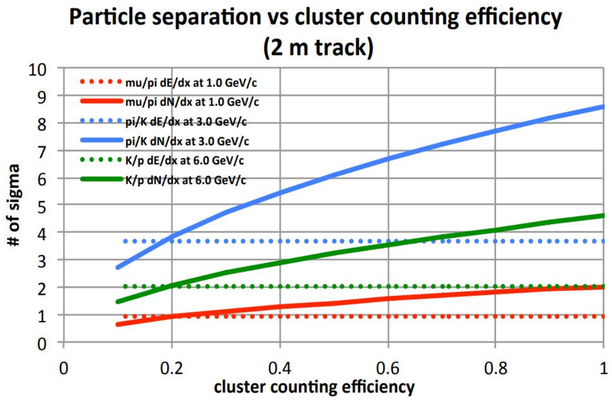

Cluster counting in simulation

Analytical calculations predict excellent K/p separation over the full range of momenta except 0.85<p<1.05 GeV

The **combination** of the **CC** and the **TOF** information provides a stable separation of K/π

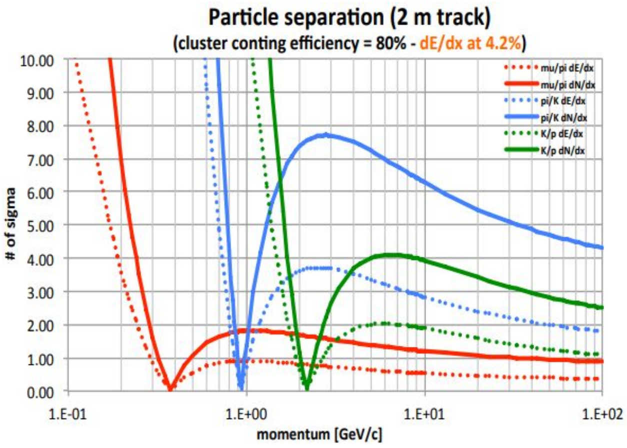

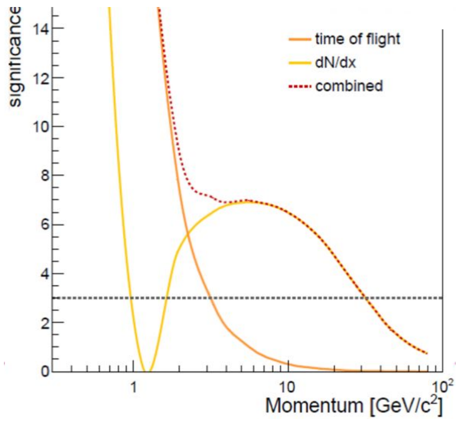

Cluster counting in simulation

Simulation with **Garfield++** and with the Garfield model ported in **GEANT4**: the particle separation, both with dE/dx and with dNcl/dx, **in GEANT4 found considerably worse** than in Garfield and the dNcl/dx Fermi plateau with respect to dE/dx is reached at lower values of βγ with a steeper slope. **Results on real data from beam tests are crucial**.

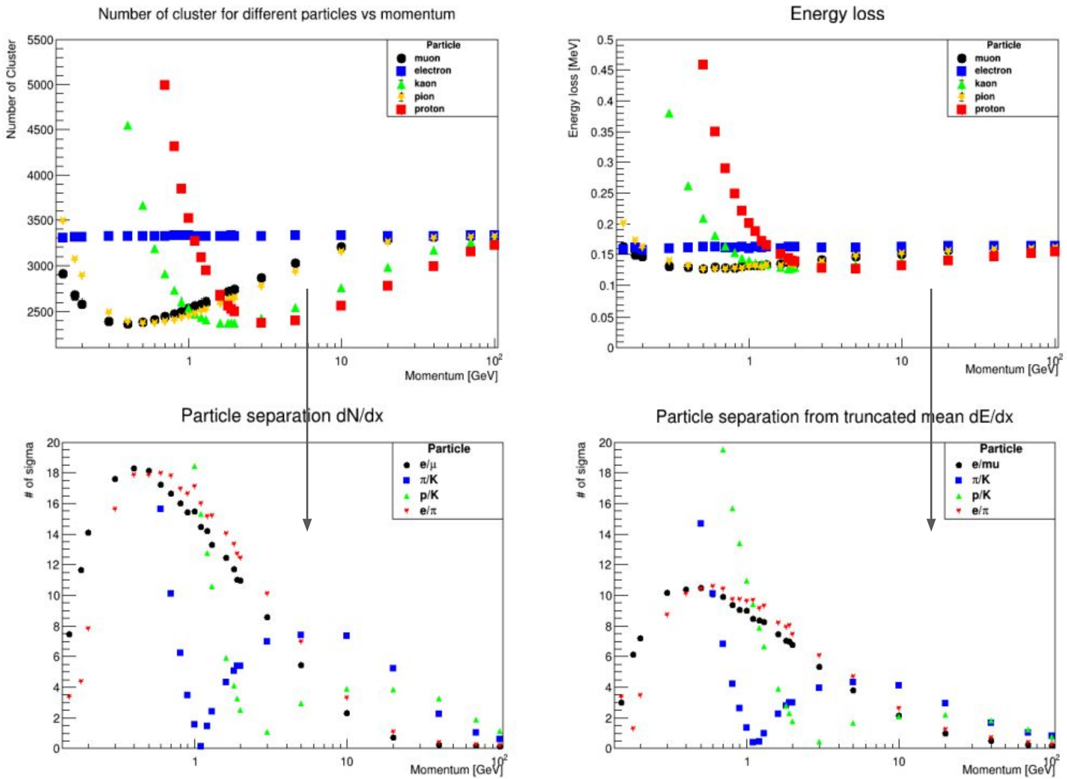

Cluster counting in testbeam

The first and second derivative algorithm (DERIV)

Requirements for a good peak candidate in the bin position [ip]:

1. Amplitude constraint:
   - Amplitude[ip]>4*rms
   - Amplitude[ip]- Amplitude[ip-1]>rms || Amplitude[ip+1]-Amplitude[ip-1]>rms
2. First derivative constraint:
   - Fderiv[ip]<σ_{der1}/2
   - Fderiv[ip-1]> σ_{der1} ||Fderiv[ip+1]<- σ_{der1}
3. Second derivative constraint:
   - Sderiv[ip]<0

0°, nominal HV+20, 90%He-10%iC_4H_{10}
Tube with 1 cm cell size and 20 μm diameter

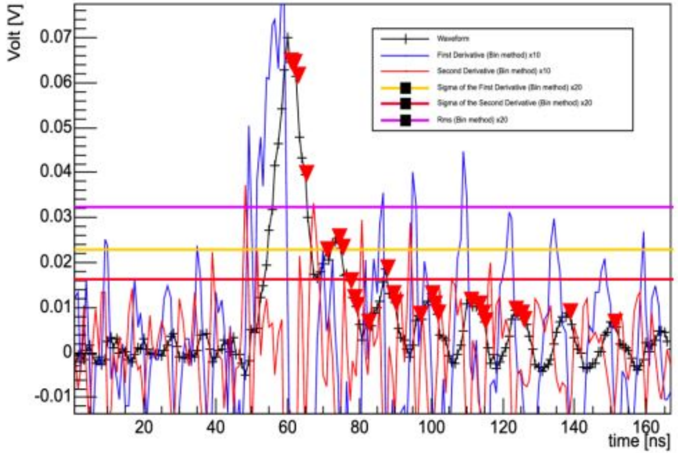

Cluster counting in testbeam

The running template algorithm (RTA)

- Define an electron pulse template based on experimental data.
- Raising and falling exponential over a fixed number of bins (Ktot).
- Digitize it (A(k)) according to the data sampling rate.
- Run over Ktot bins by comparing it to the subtracted and normalized data (build a sort of χ2).
- Define a cut on χ2.
- Subtract the found peak to the signal spectrum.
- Iterate the search.
- Stop when no new peak is found.

k	A(k)
0	0.0
1	0.269
2	1.0
3	0.744
4	0.545
5	0.390
6	0.269
7	0.175
8	0.102
9	0.044
10	0.0

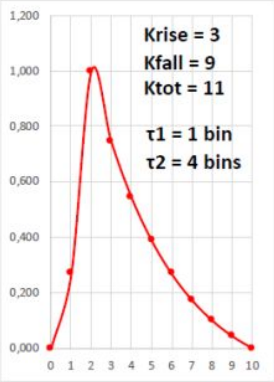

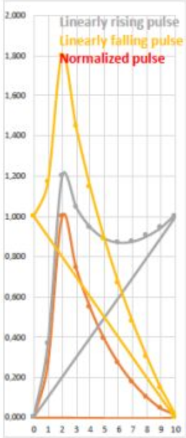

30°, nominal HV+20, 90%He-10%iC_4H_{10}
Tube with 1 cm cell size and 20 μm diameter

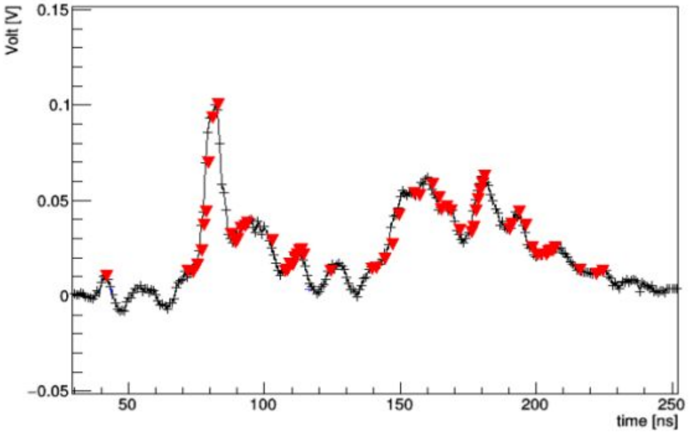

Cluster counting in testbeam

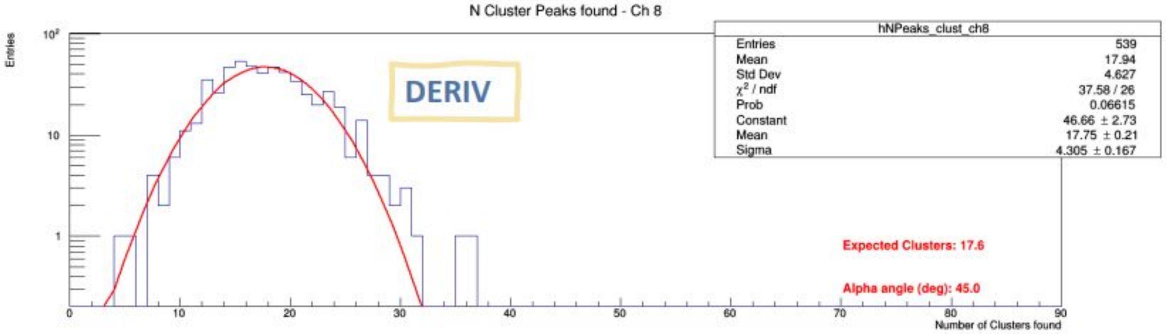

POISSONIAN DISTRIBUTION!

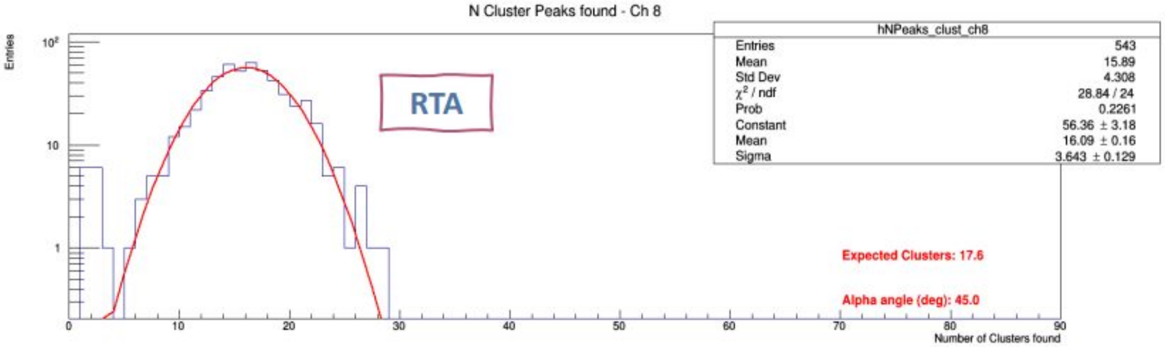

Cluster counting in testbeam

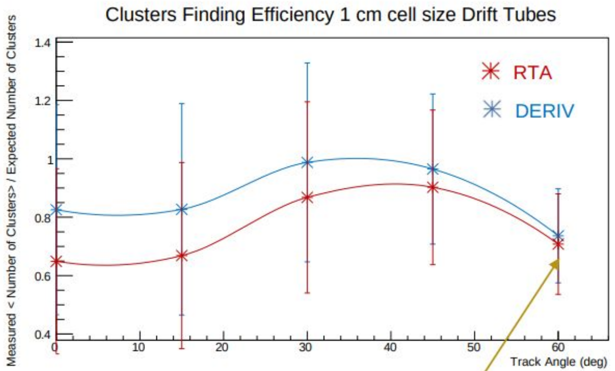

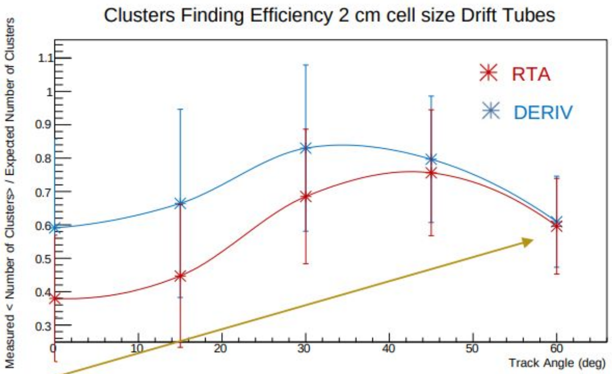

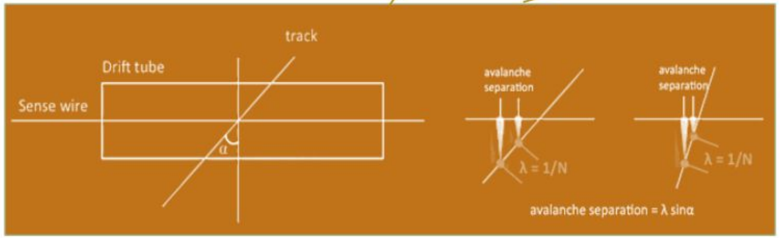

Space charge, attachment and recombination effects affect the experimental cluster counting efficiency

Tracking performance: single hit resolution

Single hit resolution is measured with the MEG-II drift chamber prototype.

A **spatial resolution of 100 μm** is achieved with this configuration

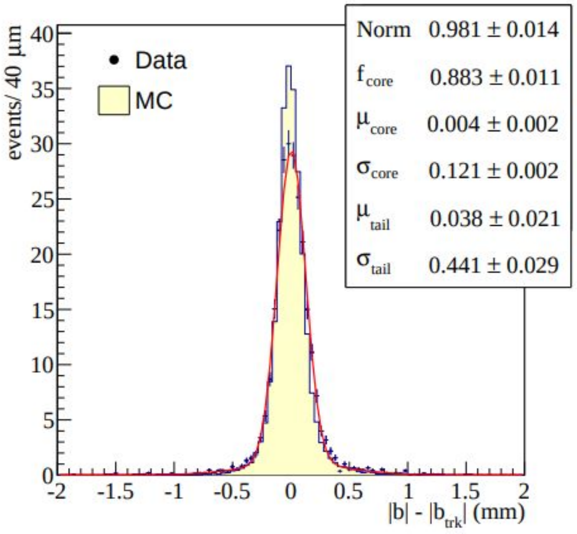

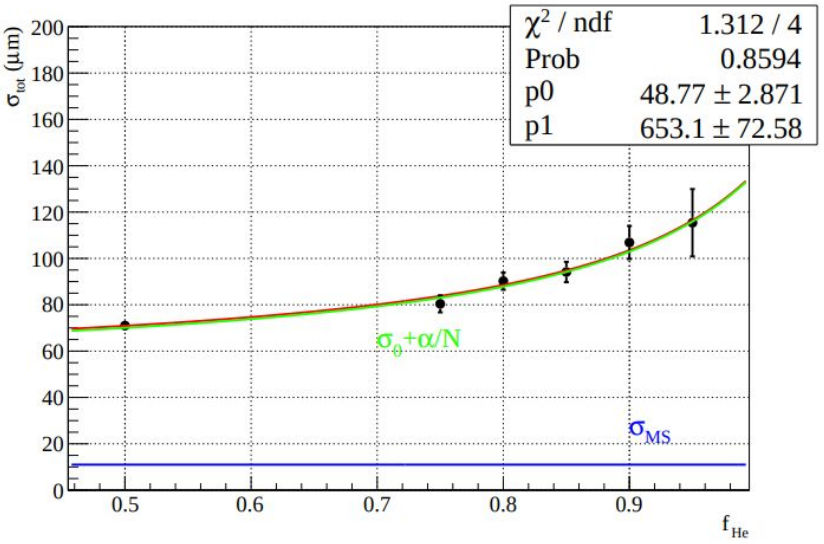

Tracking performance: single hit resolution

Assuming a 100 μm spatial resolution, the **tracking performance** are evaluated with fast simulation **combining** the DCH, the vertex and the silicon wrapper.

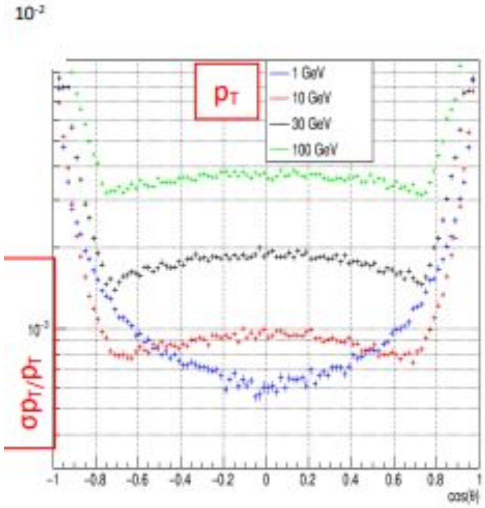

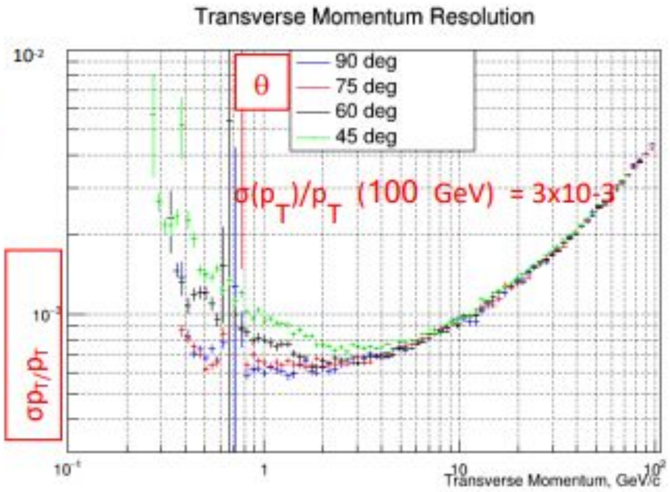

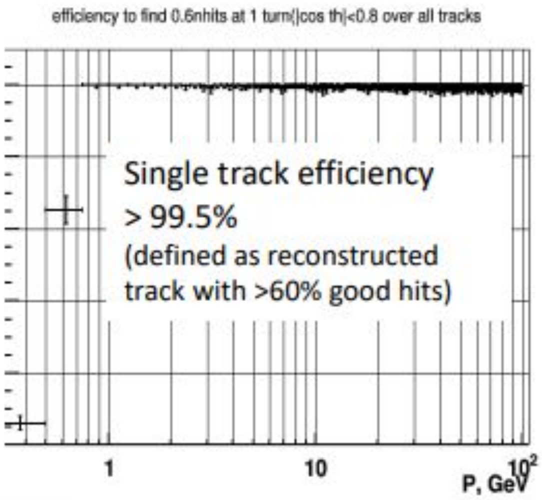

Tracking performance: single hit resolution

The large signal-to-background ratio on the one hand, and the excellent drift-chamber muon momentum resolution on the other, offer the possibility to **determine the inclusive ZH cross section and the Higgs boson mass with a statistical precision of ~1% and ~6 MeV**, respectively.

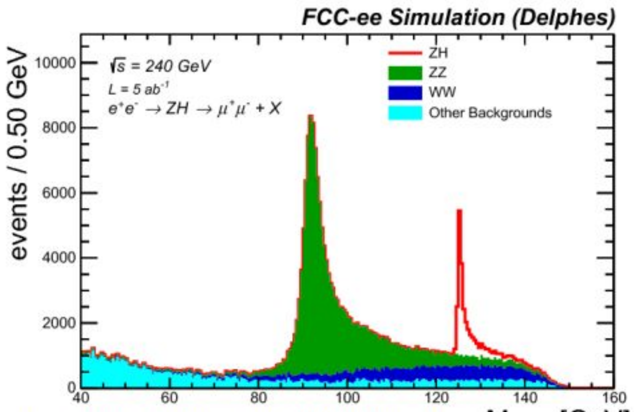

Eur.Phys.J.Plus 137 (2022) 1, 23

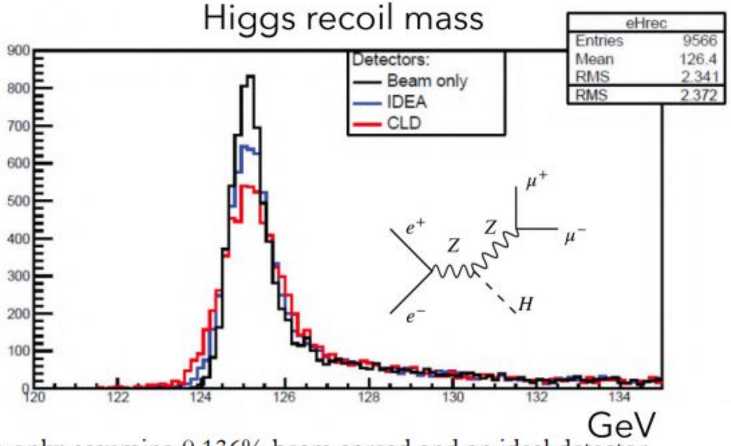

Beam only: assuming 0.136% beam spread and an ideal detector.

Machine background

A study of the **Incoherent Pair Creation** (IPC) background, expected to be the **dominant beam-induced background** in the IDEA drift chamber, was performed.

Only very few of the **primary e±** particles have a transverse momentum large enough to reach the inner **radius of the drift chamber (35 cm)**.

The majority of the hits observed in the drift chamber are thus from **secondary** particles (mainly **photons** of energy below 1 MeV) produced by scattering off the material at lower radii.

The average occupancy of the drift chamber due to this background was found to be about 0.3% (3%) per bunch crossing at 91.2 (365) GeV, with a smooth decrease by a about a factor two from low to large radii.

At the Z pole, a naive and very conservative integration **over 20 bunch crossings** – corresponding to the 400 ns maximum drift time – yields a **maximum occupancy of about 10% in the innermost** drift cells.

Machine background

Background	Average occupancy	
	$\sqrt{s}$ = 91.2 GeV	$\sqrt{s}$ = 365 GeV
e^+e^- pair background	1.1%	2.9%
$\gamma\gamma \rightarrow$ hadrons	0.001%	0.035%
Synchrotron radiation	negligible	0.2%

Based on experience from the MEG2 drift chamber, **this occupancy**, which allows over 100 hits to be recorded per track on average in the DCH, **is deemed manageable**.

The level of occupancy is actually expected to be much smaller than this conservative estimate with the use of the drift chamber **timing** measurement.

As opposed to **charged particles that leave a string** of ionisation in the drift cells they traverse, **photons are characterised by a localised energy deposition**. Signals from photons can therefore be effectively **suppressed** at the data acquisition level by requiring that at least **three ionisation** clusters appear within a time window of **50 ns**.

In addition, a **charge string with a hole longer than 100 ns can be interpreted as two separate signals**, so as to avoid the integration of any remaining photon-induced background over 20 bunch crossings, but rather integrate over a time corresponding to only four bunch crossings.

With this effective suppression of photon-induced signals, the background from IPC is expected to remain low and is unlikely to cause adverse issues for the track reconstruction. According to these considerations, the average occupancy from IPC, SR, and γγ→ hadrons is summarised in Table.

Challenges

Extremely high luminosities: large statistics (high statistical precision) - control of systematics (@10^{-5} level)

Large beam crossing angle (30mrad) very complex MDI emittance blow-up with detector solenoid field (< 2T)

Physics event rates up to 100 kHz (at Z pole) strong requirements on sub-detectors and **DAQ systems**

Bunch spacing down to 20 ns (at Z pole) "continuous" beams (no power pulsing)

More physics challenges at Z pole:

- luminosity measurement at 10^{-5} - luminometer acceptance ≈1-2 μm
- detector acceptance definition at <10^{-5} - detector hermeticity (no cracks!)
- stability of momentum measurement - stability of magnetic field wrt E_{cm} (10^{-6})
- b/c/g jets separation - flavor and τ physics - vertex detector precision
- particle identification (preserving hermeticity) - flavor physics (and rare processes)

The maximum drift time (400ns) will impose an overlap of some (20 at Z pole) bunch crossings bringing the hit occupancy to ~ 10% in the innermost drift cells. Based on MEG-II experience, this occupancy, which allows over 100 hits to be recorded per track on average in the DCH, is deemed manageable.

However, **signals from photons can be effectively suppressed** at the data acquisition level by requiring that at least three ionization clusters appear within a time window of 50 ns. In addition, **cluster signals separated by more than 100 ns** are not from the same signals, this effectively bring the **BXs pile-up from 20 to 4**

Thank you!